Journal of the Meteorological Society of Japan

EARLY ONLINE RELEASE

The DOI for this manuscript is

DOI:10.2151/jmsj.2023-025

J-STAGE Advance published date: July 19th, 2023

The final manuscript after publication will replace the preliminary version at the above DOI once it is available.

The 30-year (1987-2016) trend of strong typhoons and genesis locations found in the Japan Meteorological Agency's Dvorak reanalysis data

Yasuhiro KAWABATA[1]

Meteorological Research Institute
Japan Meteorological Agency, Tsukuba Japan

Udai SHIMADA

Meteorological Research Institute
Japan Meteorological Agency, Tsukuba Japan

and

Munehiko YAMAGUCHI

Meteorological Research Institute
Japan Meteorological Agency, Tsukuba Japan

April 22, 2023

----

1) Corresponding author: Yasuhiro Kawabata, Meteorological Research Institute, 1-1 Nagamine, Tsukuba, Ibaraki 305-0052 JAPAN.
Email: kawabata@mri-jma.go.jp

Tel: +81-29-852-9167
Fax:

Abstract

The trend of strong typhoons over the recent 30 years was analyzed using Dvorak reanalysis data from 1987 to 2016 produced by Japan Meteorological Agency. The strong typhoons were defined in this study as tropical cyclones equivalent to category 4 and 5 on the Saffir-Simpson scale. The temporal homogeneity of the Dvorak reanalysis data is expected to be much better than that of best track data. Results showed no statistically significant increasing trend in strong typhoons with large inter-annual and multi-year scale variations. Meanwhile, the spatial distribution of the genesis locations of tropical cyclones, which could influence whether or not they develop into strong typhoons, varied locally during the analysis period. The changes in genesis locations may have influenced the overall trend of strong typhoons during the analysis period. The results with the new Dvorak reanalysis data highlight the need for the accumulation of high quality data over time as well as for careful interpretation of trend analysis results seen in previous studies.

Keywords tropical cyclone; strong typhoon; Dvorak analysis; trend analysis; typhoon climatology

1. Introduction

Tropical cyclones (TCs) are weather phenomena that sometimes cause severe disasters. TCs with a maximum 10-min sustained wind speed of approximately 33 m s^{-1} (64 knots) or higher are called typhoons in the western North Pacific (WNP). Strong typhoons, which are defined in this study as TCs equivalent to category 4 or 5 on the Saffir-Simpson scale (Saffir 1973; Simpson 1974), occur every year. Whether the number of strong typhoons is increasing due to climate change is a major concern from the perspective of disaster prevention and mitigation, and also attracts a great interest of the society.

A long-term trend in the number of strong typhoons in the WNP has been investigated mainly using best track data made by Japan Meteorological Agency (JMA) or Joint Typhoon Warning Center, USA (JTWC). Since 1987, when aircraft reconnaissance ceased in the WNP, both JMA and JTWC have estimated maximum sustained wind speed (Vmax) by means of the Dvorak technique using satellite imagery (Dvorak 1984) with all other available observations. However, conversion tables from Current Intensity number (CI number) to Vmax used in the Dvorak analysis differ between JMA and JTWC. This fact resulted in significant differences in the number of strong typhoons between JMA and JTWC best track data even though different definitions of Vmax (10-min or 1-min average) were taken into account (Kamahori et al. 2006; Song et al. 2010; Schreck et al. 2014; Kossin et al. 2007; Kossin et al. 2013; Elsner 2020; Wu et al. 2021).

To resolve the issue of the difference in Vmax between JMA and JTWC, which is primarily caused by use of different conversion tables applied in the Dvorak analysis (Table 1), Mei and Xie (2016) corrected best track Vmax values estimated by JMA since 1987. Firstly, JMA's Vmax was converted to the CI number using the conversion table in the Dvorak analysis adopted in JMA (i.e., Koba et al. 1991). Then, the CI number is converted to Vmax using the conversion table adopted in JTWC (i.e., Dvorak 1984). With this correction based on the same intensity definition (1-min Vmax), it is possible to compare JMA's Vmax with JTWC's Vmax and thus compare fairly the difference in the number of strong typhoons between JMA and JTWC. Mei and Xie (2016) showed that the number of category 4 and 5 TCs significantly increased from 1977 to 2014 for JMA and JTWC. Note that in their study, JMA's Vmax was corrected with the conversion tables only after 1986 and that JMA's Vmax before 1987 was just divided by 0.88 to obtain 1-min Vmax, which is a conventional method to convert Vmax from 10-min to 1-min. Additionally, the dataset used in Mei and Xie (2016) is temporarily inhomogeneous because it was constructed using mostly aircraft observations from 1977 to 1987, and mostly Dvorak estimates from 1987 to 2014. An analysis of Mei and Xie (2016) for the period of 1987 to 2014 would likely show little trend in the number of category 4 and 5 TCs (e.g., see Fig. 1a of Mei and Xie 2016). Therefore, the positive trend from 1977 to 2014 would likely be due to fewer category 4 and 5 TCs before 1987. However, since the temporal inhomogeneity exists between before and after 1987 in the dataset of Mei and Xie (2016), it is difficult to distinguish a climatological trend from the artifact associated with changes in measurement platforms.

Table1

One approach to removing these artifacts is to reanalyze the entire record using an objective algorithm such as the one described in Kossin et al. (2013). Another approach is to reanalyze the entire record using a subjective method such as the Dvorak method. JMA has, in fact, recently produced Dvorak reanalysis data from 1987 to 2016 under a project of the Typhoon Committee (Regional Specialized Meteorological Center (RSMC) Tokyo - Typhoon Center 2023). As described in detail in section 2, Dvorak intensity (i.e., CI number) from this reanalysis data is considered to be more temporally homogeneous than best track intensity. The objective of this study is to investigate whether the number and ratio of strong typhoons are increasing in the period from 1987 to 2016. We believe that with the reanalysis data, the investigation can confirm the recent trend in typhoon intensity, although limited to the 30 years from 1987. The results of this study provide new insight into the climatology of strong typhoons.

2. Data and Method

The Dvorak technique is a method for estimating the intensity of TCs using geostationary satellite imagery (Dvorak 1984). JMA has adopted the Dvorak technique since 1987 for real-time analysis and constructing best track data. Once the CI number is determined by the Dvorak analysis, Vmax is obtained using a conversion table, which describes the statistical relationship between the CI number and Vmax (Dvorak 1975, 1984; Koba et al. 1991). The Dvorak estimated Vmax is a first guess for determining best track Vmax, which is subsequently modified based on other available observations (Kunitsugu 2012). Therefore, best track Vmax should be regarded as the "best analysis" at that time, and its quality could differ depending on the skill of TC forecasters analyzing the TC intensity and observations available (Shimada et al. 2020). Since observations used for the best track analysis have changed through the years, the best track Vmax is likely unsuitable for climatological research, especially research into changes in TC lifetime maximum intensity (LMI). However, if the Dvorak analysis is conducted in a consistent way for a long period, like advanced Dvorak Technique - Hurricane Satellite record (ADT-HURSAT) (e.g., Kossin et al. 2020), the Dvorak intensity could be suitable for trend analysis. Thus, JMA has recently performed the Dvorak reanalysis retroactive for a period of 1987 to 2016 for TCs in the WNP (i.e., 0-60°N, 100-180°E) (Nishimura et al. 2023). The reanalysis was conducted by a few skilled forecasters with consistent procedures so that the estimated Dvorak intensity (i.e., CI number) has better temporal homogeneity. Data consistency of the reanalysis data throughout the 30-year period was verified by the skilled forecasters. The differences from the real-time Dvorak technique are that the reanalysis includes the Early Dvorak Analysis (EDA) (Kishimoto et al. 2007; Kishimoto 2008) to start the Dvorak analysis at the appropriate time and avoid a delay in intensification, and that the Dvorak intensity (i.e., T number, from which the CI number is derived) in the development stage is estimated after the LMI of a TC is determined from the Data-T number (DT number) to satisfy the Dvorak constraints of T number changes. Since the LMI is analyzed first using all available satellite imagery in the reanalysis, the LMI of the Dvorak reanalysis is expected to be more reliable than that of best track data. Especially, Dvorak estimates for the CI number ranging from 5.0 to 6.5 are the highest quality estimates with a relative “sweet spot” for intensity estimation (Knaff et al. 2010).

The Dvorak reanalysis data were used in this study. Here we define “strong typhoons” as those TCs that reach at least a CI number of 6.0, which corresponds to a 10-min sustained wind speed of 90 kt (Koba et al. 1991) and a 1-min sustained wind speed of 115 kt (Dvorak 1984) (see Table 1). This intensity corresponds to Saffir-Simpson Category 4 and higher. This definition of strong typhoons is used hereafter.

For the analysis of long-term changes, regression lines and 90 % confidence intervals are used. The significance of the linear trend was tested by Mann-Kendall test (Hirsch et al. 1982) and performed the test at the 90 % confidence level. Hereafter, the 90 % confidence level is considered statistically significant.

3. Results

Fig. 1

Figure 1 shows the number of strong typhoons with a lifetime maximum CI number of 6.0 or higher and the ratio of strong typhoons to all TCs in each year from 1987 to 2016. There is no statistically significant linear trend in either the number or ratio. Similar results were obtained when TCs with a lifetime maximum CI number of 5.5 or higher, or 6.5 or higher were examined instead of strong typhoons (not shown). The 90% confidence intervals are large due to the observed interannual variability. That shows that in shorter intervals trends can be both positive and negative and that the trends are also sensitive to the endpoints of the time series being examined. The lack of an intensity trend found here is consistent with the result of Mei and Xie (2016), if their trend analysis had been performed since 1987.

Next, we compare the difference in the number of strong typhoons between the Dvorak reanalysis and the JMA best track data to look at the properties of the reanalysis dataset. Figure 2 shows the time series of the number of strong typhoons with a lifetime maximum CI number of 6.0 or higher from the Dvorak reanalysis and the number of TCs with a lifetime maximum Vmax of 90 kt (CI ~ 6.0) in Koba et al. (1991) or higher from the best track data. From 1987 to 2007, the number of strong typhoons is generally higher in the Dvorak reanalysis data than in the best track data. For 79 % of the TCs with LMI of 80$\pm$10 kt in the 1987-2007 best track data, the LMIs increased in the Dvorak reanalysis (not shown), and the positive trend seen in the best track data is not reflected in the Dvorak reanalysis data.

Fig. 2

Through interviews with forecasters in the 1990s, we infer three reasons for the LMIs in the Dvorak reanalysis being higher than those in the real-time Dvorak analyses. Note that the latter was used to construct the best track data. First, the satellite display system at that time tended to blur a small eye due to a remapping to a different spatial resolution from the original satellite data. As a result, the intensity associated with the eye pattern may have been underestimated. Second, the T numbers remained uncorrected even though subsequent analysis found that T numbers should have been higher. A related issue was poor initialization of the initial disturbance, which typically causes a delay in intensification, being "behind the curve." Consequently, the T number did not necessarily reach an appropriate T number at the peak time due to Dvorak constraints of T number increase (Dvorak 1984). This latter issue has been resolved in the Dvorak reanalysis that used EDA. Third, in the Dvorak reanalysis, the T number was retroactively corrected so that the lifetime maximum T number was determined from the DT number whenever possible. In their technical report, Nishimura et al. (2023) explained that "For TCs with a clear TC eye and clear cloud patterns, intensities up to peak values were re-analyzed as far as the beginning of tropical depression formation so that the DT number could be adopted at the peak period within Dvorak constraints."

Although the number of strong typhoons defined by a lifetime maximum CI number of 6.0 or higher showed no significant trend (Fig. 1), we investigated temporal changes per 30-year in the ratio of TCs stratified by CI number to all TCs (Fig. 3). Although there was no statistically significant linear trend at 90 % confidence level in the ratio of TCs with each lifetime maximum CI number, the following characteristics were seen: the ratio change was positive for lifetime maximum CI $\leq$ 3.0, the ratio change was negative for lifetime maximum CI = 3.5–5.5, and the ratio change varied from CI to CI for lifetime maximum CI $\geq$ 6.0.

Fig. 3

Previous studies have reported that El Niño/La Niña and the Pacific Decadal Oscillation (PDO) are related to TC activity in the WNP (Lee et al. 2012; Hong et al. 2016; Liu et al. 2019; Zhao et al. 2019; Kim et al. 2020; Yamaguchi and Maeda 2020a; Lee et al. 2021).

The temporal variation of strong typhoons may have been influenced by these phenomena. Yamaguchi and Maeda (2020b) found that the number of strong typhoons approaching the southern coast of Japan including Tokyo was increasing. These studies suggest that despite the lack of basin wide trends in strong typhoons, sub-basin variability has occurred. To explore sub-basin variability, we examined the temporal variation of the spatial distribution of strong typhoons.

Figure 4 shows the time series of annual mean genesis locations for strong typhoons with a lifetime maximum CI number of 6.0 or higher. Here, the genesis is defined as the location where the CI number of each TC first reached 2.0 or higher in the reanalyzed data. By definition, TCs with a lifetime maximum CI number less than 2.0[1] and TCs that crossed the dateline into the WNP basin were excluded in this examination. Although the linear trend in both latitude and longitude is not statistically significant, the confidence intervals of the linear regression lines show 0.2±2.0 degrees per 30-year in latitude and –4.2±5.5 degrees per 30-year in longitude, indicating that the genesis location of strong typhoons tends to shift slightly to the west (Fig.4b). Daloz and Camargo (2018) stated that the genesis location of typhoons in the WNP had shifted poleward. However, strong typhoons in the Dvorak reanalysis show no such shift in genesis location (Fig.4a).

Fig. 4

Next, we examined the temporal variation of locations where the strong typhoons first reached their LMIs (Fig. 5). Figure 5 shows that a linear increasing trend is seen in the annual mean latitude of LMI for strong typhoons at the 90 % significance level, whereas the

Fig. 5

change in the mean longitude is not statistically significant. The confidence intervals of the linear regression lines indicate 2.2±1.8 degrees per 30-year in latitude and –5.1±4.8 degrees per 30-year in longitude, indicating that the location of strong typhoons reaching their LMIs has tended to shift to the northwest. Kossin et al. (2014) found that the location of the peak maximum intensity shifts poleward, which is consistent with this study.

The results of 30-year changes in the genesis location and the LMI location of strong typhoons suggest that the distribution of strong typhoons in the WNP may have changed. Motivated by this, we examined how the ratio of strong typhoons changed locally. Figure 6 shows the genesis locations of TCs colored with the LMIs in the first half of the analysis period (1987–2001) and the second half (2002–2016). Here, the genesis location is defined as the location where the CI number of each TC first exceeded 2.0, the same as the criterion in Fig. 4. Here, TCs with a lifetime maximum CI number less than 2.0 and TCs that came into the WNP through the dateline are not shown. Table 2 presents the genesis ratio of TCs in each area (defined as areas I, II, III, and IV from 0°N to 20°N and east of 120°E in Fig. 6) to all TCs generated in all these areas including TCs that crossed the dateline into the WNP (i.e., area V), divided by three intensity groups of the lifetime maximum CI number. The genesis ratio of TCs in areas I to V to all TCs in the WNP is 63 % in the first half of the analysis period and 64 % in the second half. The ratios in the two periods are almost the same. Therefore, comparisons were made for TCs in the five areas between the two periods.

Fig. 6

Table2

The ratio of total strong typhoons (CI = 6.0–8.0) to all TCs (area I–V) is higher in the second half of the analysis period (49.6 %) than in the first half (43.7 %). This difference is due to the temporary increase in the number of TCs with a lifetime maximum CI number of 6.0 or higher from 2004 to 2007 and in 2015 (Fig. 1). Because of this irregular fluctuation, no linear increasing trend in strong typhoons was detected in Fig. 1. TCs generated in the eastern part of the WNP (i.e., 145–180°E) are characterized by a higher ratio (more than 50 %) of strong typhoons relative to the total TCs generated in the same area, compared to that in the western part of the WNP (120–130°E). In general, TCs moving westward over a long distance over the ocean have a higher chance of being exposed to an environment favorable for intensification than TCs forming close to land. This likely explains the differences in the ratio of strong typhoons between the areas seen Table 2. This feature is similar to the difference in the ratio of strong typhoons between El Niño and La Niña years. In El Niño years, TCs tend to form in more eastern locations than the climatological mean location, and in La Niña years vice versa (Chia and Ropelewski 2002; Fudeyasu et al. 2006). Meanwhile, the ratio of TCs in areas IV and V to all TCs generated in all the areas is about 6% lower in the second half of the analysis period (i.e., 9.6 %) than in the first half (15.9 %). The decrease in TC genesis in areas IV and V may be due to a change in PDO (Liu and Chan 2013). The PDO phase in the second half of the analysis period was generally negative (JMA 2022). The genesis location can change in response to positive or negative PDO phase, and the environment in the eastern part of the WNP is known to be unfavorable for TC genesis in a period of negative PDO phase (Scoccimarro et al. 2021; Cha et al. 2023).

It has also been shown the possibility that anthropogenic aerosols affected TC activity with increased aerosols in South and East Asia resulting in fewer TCs in the east of 150°E in the WNP (Murakami 2022). The decrease in the ratio of TCs generated in areas IV and V in the second half of the period (from 15.9 % to 9.6 %), accordingly, led to the decrease in the ratio of strong typhoons generated in areas IV and V by about 4 % in the second half (from 8.7 % to 4.8 %, Table 2).

In contrast, the ratio of TCs generated in area II increased in the second half of the period (from 36.5 % to 43.4 %). Furthermore, the ratio of strong typhoons in this area increased by about 8 % (from 15.9 % to 24.1 %). Recent studies have shown that oceanic condition in this area is becoming more favorable for TC development (Fudeyasu et al. 2018; Zhao et al. 2018). The increase in strong typhoons in area II is consistent with the change in the environment for TCs.

In summary, the increase in strong typhoons in areas II was partly offset by the decrease in strong typhoons in areas IV and V. It is possible that areas IV and V, where 50 % or more of TCs potentially develop into strong typhoons, have been situated in an environment unfavorable for TC genesis in the second half of the analysis period. As a result, a significant linear trend in the ratio of strong typhoons to all TCs over the 30-year period was not detected. Climatologically, it might not be surprising to see an increase in the number and/or ratio of strong typhoons due to factors such as sea surface temperature increase (Wu et al. 2020). The fact that we have not seen such a trend over the past 30 years despite this might be partly related to changes in the genesis location of strong typhoons influenced by natural climate variability such as the PDO.

4. Conclusion

We investigated the long-term temporal variation of strong typhoons with a lifetime maximum CI number of 6.0 or higher for the recent 30-year period (1987–2016), using Dvorak reanalysis data provided by JMA, which are considered to be more suitable for trend analyses than best track data from the perspective of temporal homogeneity. The results showed no statistically significant trend in the number of strong typhoons and the ratio of strong typhoons to all TCs over the 30-year period, with large inter-annual and multi-year scale variations. The result is consistent with that of Mei and Xie (2016) if their analysis period started in 1987, when aircraft observations ended. In addition, we examined the spatial distribution of strong typhoons, and their genesis (CI ≥ 2.0) locations. Whereas the ratio of strong typhoons that were generated in the area near the dateline in the WNP to all TCs in analysis area decreased in the second half of the analysis period, the ratio of strong typhoons that were generated in the western part of the WNP increased in the second half. The second half of the 1987-2016 analysis period experienced a negative PDO phase, and the associated unfavorable environment for TC genesis may have affected TC trends in the WNP. Results shown here highlight the need for high quality and temporally consistent datasets for climatological studies, especially those analyzing trends, as well as for careful interpretation of trend analysis results seen in previous studies.

Data Availability Statement

TC best track data are available online at the RSMC website (https://www.jma.go.jp/jma/jma-eng/jma-center/rsmc-hp-pub-eg/trackarchives.html). Information regarding the use of Dvorak reanalysis data will be available online on the RSMC Tokyo website. (https://www.jma.go.jp/jma/jma-eng/jma-center/rsmc-hp-pub-eg/RSMC_HP.htm).

Acknowledgments

The authors thank the editor Dr. Masuo Nakano and the reviewers, Dr. John Knaff and Mr. Buck Sampson, for useful comments and suggestions. The authors also thank Dr. Masato Sugi and Mr. Shuji Nishimura for insightful discussions and JMA for providing the Dvorak reanalysis data. The opinions in this paper are those of the authors and should not be regarded as official views of JMA.

References

Cha, Y., J. Choi, and J.-B. Ahn, 2023: Interdecadal changes in the genesis activity of the first tropical cyclones over the western North Pacific from 1979 to 2016. *Clim. Dyn.*, **60**, 1885–1906, doi:10.1007/s00382-022-06382-2.

Chia, H. H., and C. F. Ropelewski, 2002: The interannual variability in the genesis location of tropical cyclones in the northwest Pacific. *J. Climate*, **15**, 2934–2944.

Daloz, A. S., and S. J. Camargo, 2018: Is the poleward migration of tropical cyclone maximum intensity associated with a poleward migration of tropical cyclone genesis? *Climate Dyn*., **50**, 705–715, doi:10.1007/s00382-017-3636-7.

Dvorak, V. F., 1975: Tropical Cyclone Intensity Analysis and Forecasting from Satellite Imagery. *Mon. Wea. Rev.*, **103**, 420–430, doi:10.1175/1520-0493(1975)103<0420:TCIAAF>2.0.CO;2.

Dvorak, V. F., 1984: Tropical cyclone intensity analysis using satellite data. *NOAA Tech. Rep.*, **11**, 45pp.

Elsner, J. B., 2020: Continued increases in the intensity of strong tropical cyclones. *Bull. Amer. Meteor. Soc.*, **101**, E1301–E1303, doi:10.1175/bams-d-19-0338.1.

Fudeyasu, H., S. Iizuka, and T. Matsuura, 2006: Impact of ENSO on landfall characteristics of tropical cyclones over the western North Pacific during the summer monsoon season. *Geophys. Res. Lett.*, **33**, L21815, doi:10.1029/2006GL027449.

Fudeyasu, H., K. Ito, and Y. Miyamoto, 2018: Characteristics of tropical cyclone rapid intensification over the western North Pacific. *J. Climate*, **31**, 8917–8930, doi:10.1175/JCLI-D-17-0653.1.

Hirsch, R. M., J. R. Slack, and R. A. Smith, 1982: Techniques of trend analysis for monthly water quality data. *Water Resour. Res.*, **18**, 107–121.

Hong, C.-C., Y.-K. Wu, and T. Li, 2016: Influence of climate regime shift on the interdecadal change of tropical cyclone activity over Pacific Basin during middle to late 1990s. *Climate Dyn.*, **47**, 2587–2600, doi:10.1007/s00382-016-2986-x.

Japan Meteorological Agency, 2022: El Niño/La Niña and PDO (Pacific Decadal Oscillation). *Climate Change Monitoring Report 2021*, 66-67.

Kamahori, H., N. Yamazaki, N. Mannoji, and K. Takahashi, 2006: Variability in intense tropical cyclone days in the western North Pacific. *SOLA*, **2**, 104−107, doi:10.2151/sola.2006-027.

Kim, H. K., K. H. Seo, S. W. Yeh, et al., 2020: Asymmetric impact of Central Pacific ENSO on the reduction of tropical cyclone genesis frequency over the western North Pacific since the late 1990s. *Clim. Dyn.*, **54**, 661–673, doi:10.1007/s00382-019-05020-8.

Kishimoto, K., T. Nishigaki, S. Nishimura, and Y. Terasaka, 2007: Comparative study on organized convective cloud systems detected through early stage Dvorak analysis and tropical cyclones in early developing stage in the western North Pacific and the South China Sea. *RSMC Tokyo – Typhoon Center Technical Review*, **9**, 1−14. [Available online at https://www.jma.go.jp/jma/jma-eng/jma-center/rsmc-hp-pub-eg/techrev/text9-2.pdf.]

Kishimoto, K., 2008: Revision of JMA’s early stage Dvorak analysis and its use to analyze tropical cyclones in the early developing stage. *RSMC Tokyo – Typhoon Center Technical Review*, **10**, 1−12. [Available online at https://www.jma.go.jp/jma/jma-eng/jma-center/rsmc-hp-pub-eg/techrev/text10-1.pdf.]

Knaff, J. A., D. P. Brown, J. Courtney, G. M. Gallina, and J. L. Beven II, 2010: An evaluation of Dvorak technique-based tropical cyclone intensity estimates. *Wea. Forecasting*, **25**, 1362−1379.

Koba, H., T. Hagiwara, S. Osano, and S. Akashi, 1991: Relationship between CI number and minimum sea level pressure/maximum wind speed of tropical cyclones. *Geophys. Mag.*, **44**, 15−25.

Kossin, J. P., K. R. Knapp, D. J. Vimont, R. J. Murnane, and B. A. Harpar, 2007: A globally consistent reanalysis of hurricane variability and trends. *Geophys. Res. Lett.*, **34**, L04815, doi:10.1029/2006GL028836.

Kossin, J. P., T. L. Olander, and K. R. Knapp, 2013: Trend analysis with a new global record of tropical cyclone intensity. *J. Climate*, **26**, 9960−9976, doi:10.1175/JCLI-D-13-00262.1.

Kossin, J. P., K. A. Emanuel, and G. A. Vecchi, 2014: The poleward migration of the location of tropical cyclone maximum intensity. *Nature*, **509**, 349–352, doi:10.1038/nature13278.

Kossin, J. P., K. R. Knapp, T. L. Olander, and C. S. Velden, 2020: Global increase in major tropical cyclone exceedance probability over the past four decades. *Proc. Natl. Acad. Sci.*

U.S.A., **117**, 11975−11980, doi: 10.1073/pnas.1920849117.

Kunitsugu, M., 2012: Tropical cyclone information provided by the RSMC Tokyo-Typhoon Center. *Trop. Cyclone Res. Rev.*, **1**, 51−59, doi:10.6057/2012TCRR01.06.

Lee, H. S., T. Yamashita, and T. Mishima, 2012: Multi-decadal variations of ENSO, the Pacific decadal oscillation and tropical cyclones in the western North Pacific. *Prog. Oceanogr.*, **105**, 67–80, doi:10.1016/j.pocean.2012.04.009.

Lee, M., T. Kim, D.-H. Cha, S.-K. Min, D.-S. R. Park, S.-W. Yeh, and J. C. L. Chan, 2021: How does Pacific Decadal Oscillation affect tropical cyclone activity over Far East Asia? *Geophys. Res. Lett.*, **48**, e2021GL096267. doi:10.1029/2021GL096267.

Liu, K. S., and J. C. L. Chan, 2013: Inactive period of western North Pacific tropical cyclone activity in 1998–2011. *J. Climate*, **26**, 2614–2630, doi:10.1175/JCLI-D-12-00053.1.

Liu, C., W. Zhang, X. Geng, M. F. Stuecker, and F.-F. Jin, 2019: Modulation of tropical cyclones in the southeastern part of western North Pacific by tropical Pacific decadal variability. *Clim. Dyn.*, **53**, 4475–4488, doi:10.1007/s00382-019-04799-w.

Mei, W., and S. P. Xie, 2016: Intensification of landfalling typhoons over the northwest Pacific since the late 1970s. *Nat. Geosci.*, **9**, 753−757.

Murakami, H., 2022: Substantial global influence of anthropogenic aerosols on tropical cyclones over the past 40 years. *Sci. Adv.*, **8**, eabn9493, doi:10.1126/sciadv.abn94

Nishimura, S., M. Sasaki, N. Nonaka, M. Ueno, Y. Mochizuki, and M. Miura, 2023: The Japan Meteorological Agency's Dvorak re-analysis data. *RSMC Tokyo – Typhoon Center*

Technical Review (in press). [Will be available online at https://www.jma.go.jp/jma/jma-eng/jma-center/rsmc-hp-pub-eg/techrev.htm.]

RSMC Tokyo - Typhoon Center, 2023: Activities of the RSMC Tokyo - Typhoon Center in 2022. ESCAP/WMO Typhoon Committee, Fifty fifth Session. [Available online at https://typhooncommittee.org/55th/docs/item%207/7.1.Review_RSMC_Activities_2022_20230213.pdf.]

Saffir, H. S., 1973: Hurricane wind and storm surge. *Mil. Eng.*, **423**, 4–5.

Schreck, C. J., K. R. Knapp, and J. P. Kossin, 2014: The impact of best track discrepancies on global tropical cyclone climatologies using IBTrACS. *Mon. Wea. Rev.*, **142**, 3881−3899, doi:10.1175/MWR-D-14-00021.1.

Scoccimarro, E., Villarini, G., Gualdi, S., & Navarra, A. 2021. The Pacific Decadal Oscillation modulates tropical cyclone days on the interannual timescale in the North Pacific Ocean. *J. Geophys. Res.: Atmospheres*, **126**, e2021JD034988, doi:10.1029/2021JD034988

Shimada, U., M. Yamaguchi, and S. Nishimura, 2020: Is the number of tropical cyclone rapid intensification events in the western North Pacific increasing? *SOLA*, **16**, 1−5, doi:10.2151/sola.2020-001.

Simpson, R. H., 1974: The hurricane disaster – Potential scale. *Weatherwise*, **27**, 169–186, doi:10.1080/00431672.1974.9931702.

Song, J., Y. Wang, and L. Wu, 2010: Trend discrepancies among three best track data sets of western North Pacific tropical cyclones. *J. Geophys. Res.*, **115**, D12128, doi:10.1029/2009JD013058.

Yamaguchi, M., and S. Maeda, 2020a: Slowdown of typhoon translation speeds in mid-latitudes in September influenced by the Pacific Decadal Oscillation and global warming. *J. Meteor. Soc. Japan*, **98**, 1321–1334, doi:10.2151/jmsj.2020-068.

Yamaguchi, M., and S. Maeda, 2020b: Increase in the number of tropical cyclones approaching Tokyo since 1980. *J. Meteor. Soc. Japan*, **98**, 775–786, doi:10.2151/jmsj.2020-039.

Wu, Z., C. Jiang, M. Conde, J. Chen, and B. Deng, 2020: The long-term spatiotemporal variability of sea surface temperature in the northwest Pacific and China offshore. *Ocean. Sci.*, **16**, 83-97, doi:10.5194/os-16-83-2020.

Wu, X., X.-H. Yan, Y. Li, H. Mei, Y.-A. Liou, and G. Li, 2021: Climatic variation of maximum intensification rate for major tropical cyclones over the Western North Pacific. *Atmosphere*, **12**, 494. doi:10.3390/atmos12040494.

Zhao H, X. Duan, G. B. Raga, P. Klotzbach, 2018: Changes in characteristics of rapidly intensifying western North Pacific tropical cyclones related to climate regime shifts. *J. Climate*, **31**, 8163–8179, doi: 10.1175/JCLI-D-18-0029.1.

Zhao, H., and C. Wang, 2019: On the relationship between ENSO and tropical cyclones in the western North Pacific during the boreal summer. *Clim. Dyn.*, **52**, 275–288, doi:10.1007/s00382-018-4136-0.

List of Figures

Fig. 1 Time series of (a) the number of strong typhoons with a lifetime maximum CI number of 6.0 or higher and (b) the ratio of strong typhoons to all TCs in each year for the Dvorak reanalysis. The linear regression and the 90 % confidence interval around the linear regression line are shown in red and orange, respectively.

Fig. 2 Time series of the number of strong typhoons with a lifetime maximum CI number of 6.0 or higher for the Dvorak reanalysis and a maximum sustained wind speed of 90 kt or higher for the best track. The thin lines represent the regression lines.

Fig. 3 Temporal changes per 30-year in the ratio of TCs stratified by a lifetime maximum CI number for the Dvorak reanalysis. Note that all temporal changes are not statistically significant at 90 % confidence level.

Fig. 4 Time series of (a) the latitude and (b) the longitude of mean genesis location for strong typhoons with a lifetime maximum CI number of 6.0 or higher for the Dvorak reanalysis. The linear regression and the 90 % confidence interval around the linear regression line are shown in red and orange, respectively.

Fig. 5 Time series of (a) the latitude and (b) the longitude of mean location at peak intensity for strong typhoons with a lifetime maximum CI number of 6.0 or higher for the Dvorak reanalysis. The linear regression and the 90 % confidence interval around the linear regression line are shown in red and orange, respectively.

Fig. 6 Distribution of genesis location of TCs with a lifetime maximum CI number showing in colors (a) from 1987 to 2001 and (b) from 2002 to 2016 for the Dvorak reanalysis. Red squares represent the areas discussed in Table 2. Note region V in Table 2 is east of the dateline and not shown here.

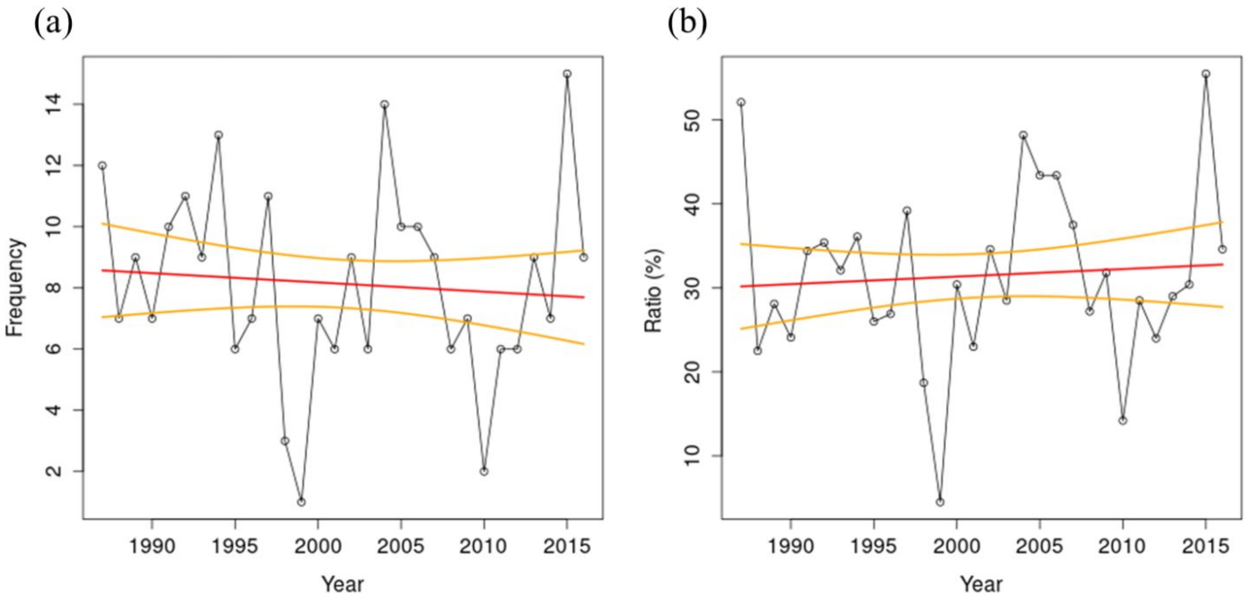

Fig. 1 Time series of (a) the number of strong typhoons with a lifetime maximum CI number of 6.0 or higher and (b) the ratio of strong typhoons to all TCs in each year for the Dvorak reanalysis. The linear regression and the 90 % confidence interval around the linear regression line are shown in red and orange, respectively.

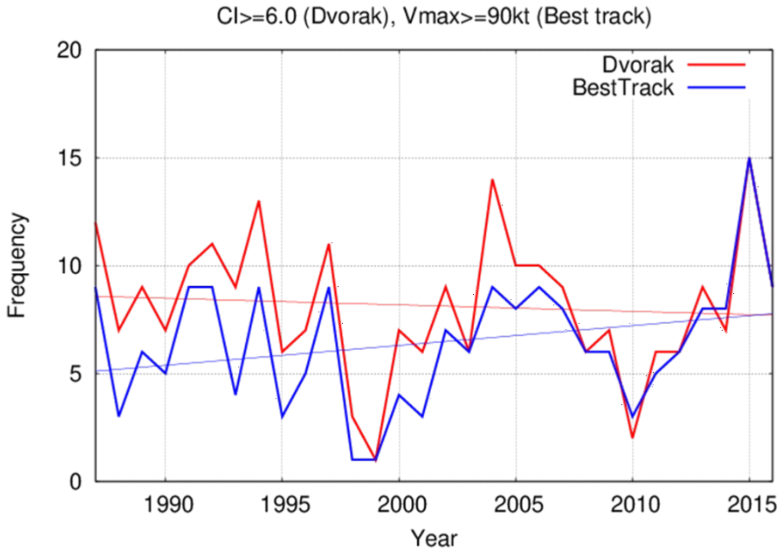

Fig. 2 Time series of the number of strong typhoons with a lifetime maximum CI number of 6.0 or higher for the Dvorak reanalysis and a maximum sustained wind speed of 90kt or higher for the best track. The thin lines represent the regression lines.

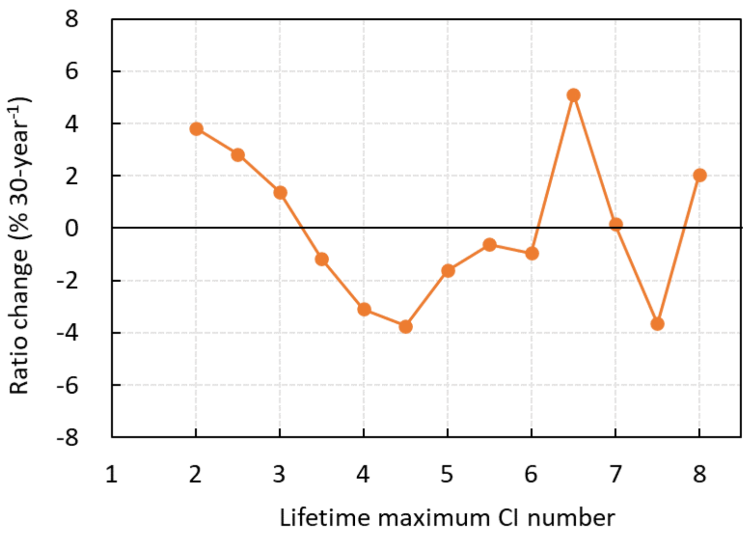

Fig. 3 Temporal changes per 30-year in the ratio of TCs stratified by a lifetime maximum CI number for the Dvorak reanalysis. Note that all temporal changes are not statistically significant at 90 % confidence level.

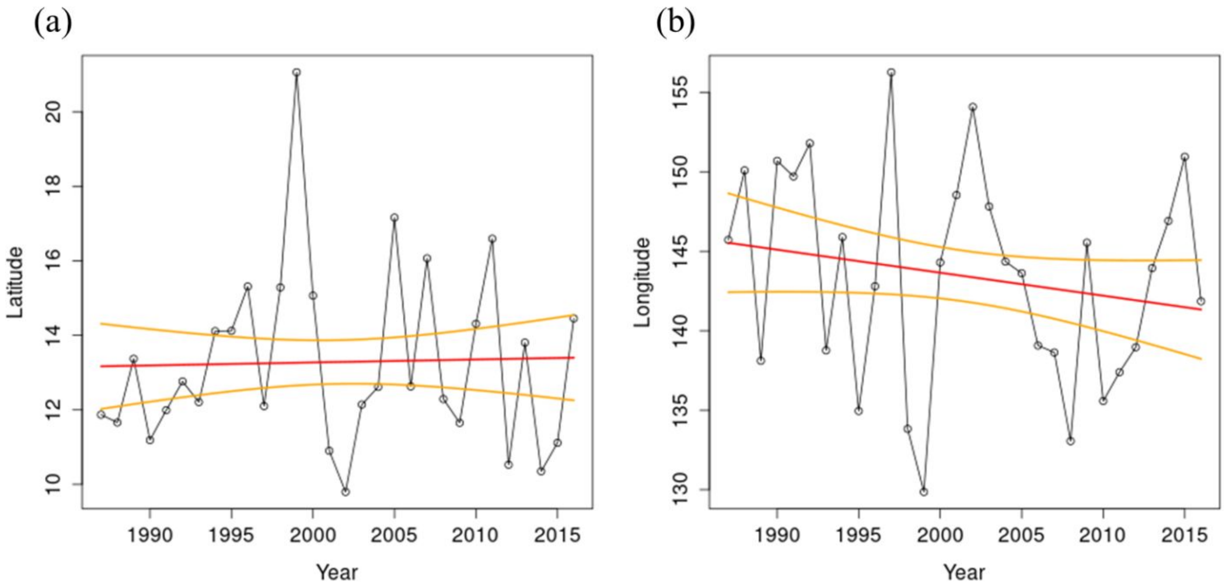

Fig. 4 Time series of (a) the latitude and (b) the longitude of mean genesis location for strong typhoons with a lifetime maximum CI number of 6.0 or higher for the Dvorak reanalysis. The linear regression and the 90 % confidence interval around the linear regression line are shown in red and orange, respectively.

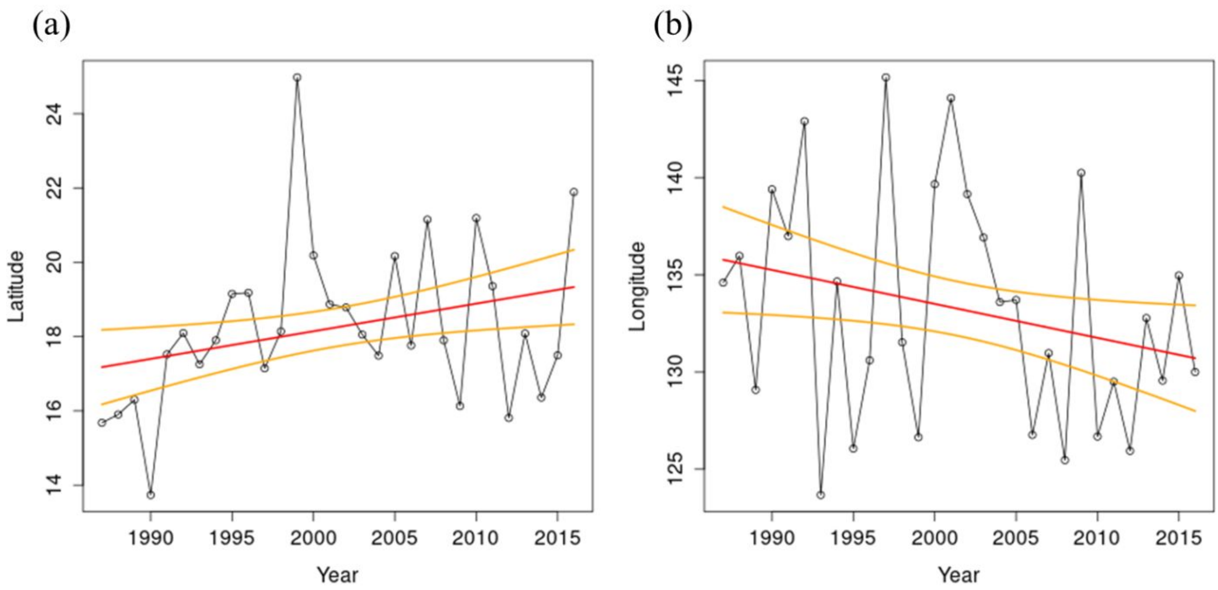

Fig. 5 Time series of (a) the latitude and (b) the longitude of mean location at peak intensity for strong typhoons with a lifetime maximum CI number of 6.0 or higher for the Dvorak reanalysis. The linear regression and the 90 % confidence interval around the linear regression line are shown in red and orange, respectively.

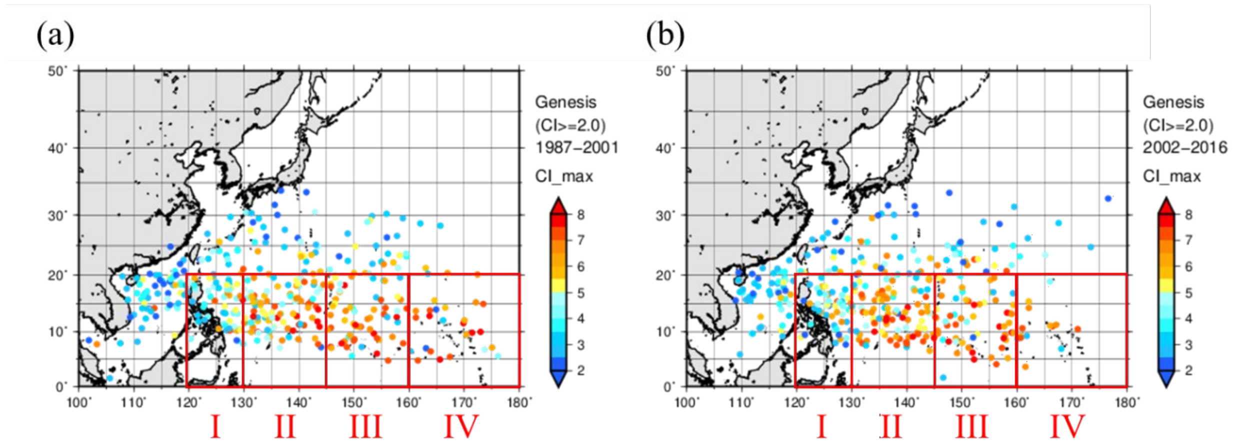

Fig. 6 Distribution of genesis location of TCs with a lifetime maximum CI number showing in colors (a) from 1987 to 2001 and (b) from 2002 to 2016 for the Dvorak reanalysis. Red squares represent the areas discussed in Table 2. Note region V in Table 2 is east of the dateline and not shown here.

List of Tables

Table 1 Dvorak conversion tables of the relationship between CI number and maximum sustained wind speed for JMA and JTWC.

Table 2 Genesis ratio of TCs in each area (defined as areas I, II, III, and IV from 0°N to 20°N and east of 120°E in Fig. 6) to all TCs generated in all these areas including TCs that came from the western longitude area (i.e., area V), divided by three intensity groups of the lifetime maximum CI number. The brackets indicate number of samples.

Table 1 Dvorak conversion tables of the relationship between CI number and maximum sustained wind speed for JMA and JTWC.

CI number	Koba et al. (1991)	Dvorak (1984)
	10-min Vmax (kt)	1-min Vmax (kt)
1.0	22	25
1.5	29	25
2.0	36	30
2.5	43	35
3.0	50	45
3.5	57	55
4.0	64	65
4.5	71	77
5.0	78	90
5.5	85	102
6.0	93	115
6.5	100	127
7.0	107	140
7.5	115	155
8.0	122	170

Table 2 Genesis ratio of TCs in each area (defined as areas I, II, III, and IV from 0°N to 20°N and east of 120°E in Fig. 6) to all TCs generated in all these areas including TCs that came from the western longitude area (i.e., area V), divided by three intensity groups of the lifetime maximum CI number. The brackets indicate number of samples.

1987-2001	Latitude (° N)	0-20					Total
	Longitude (° E)	120-130 I	130-145 II	145-160 III	160-180 IV	180- V	
CI = 2.0-3.5		8.3% (21)	7.1% (18)	4.0% (10)	1.6% (4)	2.4% (6)	23.4% (59)
CI = 4.0-5.5		10.7% (27)	13.5%(34)	5.6% (14)	1.6% (4)	1.6% (4)	32.9% (83)
CI = 6.0-8.0		4.0% (10)	15.9% (40)	15.1% (38)	6.3% (16)	2.4% (6)	43.7% (110)
Total		23.0% (58)	36.5% (92)	24.6% (62)	9.5% (24)	6.3% (16)	(252)

2002-2016	Latitude (° N)	0-20					Total
	Longitude (° E)	120-130 I	130-145 II	145-160 III	160-180 IV	180- V	
CI = 2.0-3.5		9.6% (22)	7.0% (16)	3.9% (9)	1.3% (3)	0.4% (1)	22.4% (51)
CI = 4.0-5.5		7.5% (17)	12.3% (28)	5.3% (12)	1.3% (3)	1.8% (4)	28.1% (64)
CI = 6.0-8.0		3.9% (9)	24.1% (55)	16.7% (38)	3.5% (8)	1.3% (3)	49.6% (113)
Total		21.1% (48)	43.4% (99)	25.9% (59)	6.1% (14)	3.5% (8)	(228)